Int J Adv Manuf Technol (2017) 89:3337–3348
DOI 10.1007/s00170-016-9255-3

ORIGINAL ARTICLE

Estimation of the active grains load in different kinematic variations of the internal cylindrical grinding process

Krzysztof Nadolny [1]

Received: 16 March 2014 / Accepted: 1 August 2016 / Published online: 20 August 2016

Abstract This article presents indexes referred to in literature and used when describing the working conditions of abrasive grains in internal cylindrical grinding processes: equivalent chip thickness h_{eq}, material removal rate Q_w and the proper grinding material removal rate Q'_w, as well as the average cross-section of the cut layer A_D. From consideration of these indexes, it became apparent that there was a need to develop a new index which would synthetically combine all of the key grinding parameters, as well as the geometric structure of the grinding wheel active surface. A new index was defined, marked as SI_Q (synthetic index of single abrasive grain material removal rate), in which the material removal rate Q_w was related to the number of active grains on the grinding wheel surface and the converse speed ratio $q = v_s/v_w$. The work presents example calculations and charts detailing the changes within the SI_Q index values for the following kinematic variations of internal cylindrical grinding processes: traverse grinding, reciprocating grinding, plunge grinding and plunge grinding with grinding wheel oscillations. The work includes an analytical and experimental example of how the SI_Q index can be used to determine the grinding parameters within which the grain load remained at a similar level in various kinematic variations of the grinding process. The analyses performed show that application of the proposed index allows for: a comparison of various kinematic variations of internal cylindrical grinding, the selection of machining parameters in instances where the grinding kinematics may need to be altered, the necessity for maintaining the active grains load at the same level, determination of the changes of the active cutting vertexes load during the functioning of select machining parameters, and the comparison of grinding wheels with a variety of active surface geometric structures.

Keywords Internal cylindrical grinding · Traverse grinding · Reciprocating grinding · Plunge grinding · Active grains load · Material removal rate

1 Introduction

Internal cylindrical grinding is one of the most difficult types of grinding process due to the long path of contact between the grinding wheel and the workpiece. This aspect hampers the advancement of the cooling liquid to the grinding zone and has a negative impact on the removal of the ground products [1–4]. Therefore, optimization of the grinding wheel construction and process parameters is essential for obtaining better machining results. One criterion for the selection of grinding parameters is the prolongation of the grinding wheel durability period. For grinding wheels using grains with microcrystalline structure, prolonged durability is usually obtained through the effective self-sharpening of the abrasive grains, which involves gradual chipping of microzones on the dull active vertexes to reveal new, sharp edges [1–5]. The main factor that determines the occurrence and intensity of the self-sharpening process is the load of the active cutting vertexes.

Various indexes describing the grinding wheel operating conditions during machining are available from the literature. The most frequent ones include equivalent chip thickness h_{eq}, material removal rate Q_w, material removal rate per unit of active grinding wheel width Q'_w, and average cross-section of the cut layer A_D [1–4, 6–10]. Table 1 shows the relationship

✉ Krzysztof Nadolny
krzysztof.nadolny@tu.koszalin.pl

[1] Department of Production Engineering, Faculty of Mechanical Engineering, Koszalin University of Technology, Raclawicka 15-17, 75-620 Koszalin, Poland

Table 1 Parameters defining the conditions of the material removal process during internal cylindrical grinding [1–4, 6–10]

	Traverse grinding	Reciprocating grinding	Plunge grinding	Plunge grinding with osccillations
Equivalent chip thickness h_{eq}, μm	$h_{eq} = \frac{a_f}{\lvert q \rvert} tg\,\chi$ (1)	$h_{eq} = \frac{\pi \cdot d_w \cdot a_e \cdot v_{fa}}{v_s \cdot T}$ (2)	$h_{eq} = \frac{\pi \cdot d_w \cdot v_{fr}}{v_s}$ (3)	
Material removal rate Q_w, mm^3/s	$Q_w = \pi \cdot d_w \cdot a_e \cdot a_f \cdot n_w$ (4) where: $a_f \cdot n_w = v_{fa}$ (5)		$Q_w = \pi \cdot d_w \cdot a_a \cdot a_e \cdot n_w$ (6) where: $a_e \cdot n_w = v_{fr}$ (7)	
Material removal rate per unit of active grinding wheel width Q'_w, mm^3/s·mm	$Q'w = \pi \cdot d_w \cdot n_w \cdot a_f \cdot tgx$ (8)	$Q'_w = \frac{\pi \cdot d_w \cdot n_w \cdot a_f \cdot a_e}{T}$ (9)	$Q'_w = \frac{\pi \cdot d_w \cdot n_w \cdot a_a \cdot a_e}{T}$ (10)	
Average area of cut layer cross-section A_D, μm^2	$A_D = \frac{v_w}{v_s} \frac{1}{N_a} \sqrt{\frac{a_e}{d_{eq}}}$ (11)	where:	$d_{eq} = \frac{d_w \cdot d_s}{d_w - d_s}$ (12)	

Nomenclature: a_a axial engagement (mm), a_e working engagement (mm), a_f feed engagement (mm), d_{eq} equivalent grinding wheel diameter (mm), d_s grinding wheel diameter (mm), d_w workpiece diameter (mm), n_w workpiece rotational speed (min^{-1}); N_a active grain count (mm^{-2}), v_{fa} axial table feed speed (mm/s), v_{fr} radial table feed speed (mm/s), v_s grinding wheel peripheral speed (m/s), v_w workpiece peripheral speed (m/s), T grinding wheel total height in axial direction (mm), q speed ratio (−), χ angle of conic chamfer (°)

between these parameters for the considered kinematic variations of the internal cylindrical grinding process.

None of the indexes in Table 1 consider a sufficient number of grinding parameters to allow comparison of the working conditions of the abrasive grains between various grinding wheels and internal cylindrical grinding parameters (and also considering the specific character of various kinematic types of this process). To compare the material removal conditions for various grinding wheels that, for example, differ in the abrasive grain size, it is necessary to consider the parameters describing the number of active grains on the grinding wheel active surface (GWAS). This is provided solely by parameter A_D, which defines the average cross-section of the cut layer. However, in its present form (11), A_D parameter does not allow to recreate exactly the same operating conditions of the abrasive grains in various grinding kinematics, as it is not dependent on the feed speed (v_{fa} or v_{fr}).

In view of the above problem, an attempt was made to define a new index describing the active grains load in the internal cylindrical grinding process so that a comparison of kinematic variations could be possible. This index would also consider the geometrical structure of the surface (GSS) of the grinding wheel. The comparison should be unequivocal and easy to apply, not only in laboratory research but also in industries, particularly where it is necessary to know the influence of various parameters on the abrasive grains operating conditions and the resulting intensity of grinding wheel wear. Application of a proper index would allow a single grinding wheel characteristic to recreate a comparable grains load in a different grinding procedure by proper selection of the grinding parameters. This would also allow the comparison between grinding wheels with diverse GWAS geometric structure and therefore facilitate the reconstruction of the desired operating conditions, including wear and self-sharpening of the GWAS, through the careful selection of the most important machining parameters.

To define the new index, a normalized grinding wheel material removal rate Q_w expressed in mm$_3$/s was used, determining the material removal V_w per time unit [6]. Based on this rate and the number of active grains that participate in material removal, a synthetic index of a single abrasive grain material removal rate was developed, marked as SI_Q and expressed in cubic micrometers per second.

2 Material removal rate Q_w

To establish the precise grinding material removal rate, the different kinematics of processes such as traverse grinding [7, 8, 11–13], reciprocal grinding, plunge grinding, and plunge grinding with oscillations have to be considered. In this way, the active grains load on the GWAS in each variant of the internal cylindrical grinding process can be assessed. The literature available provides descriptions of the temporary material removal rate in different internal cylindrical grinding kinematic variants [1–4, 6–10].

Technically, there is a difference between the rate determined using the formulas quoted in the literature and the actual material removal rate, described as the removed material's volume V_w after completion of the grinding operation in time t. This discrepancy is usually caused by the grinding wheel coasting c_s, which prolongs the factual machining time. In internal port grinding processes, the coasting (usually with a value of 30 % of the grinding wheel height T on each side of the portal) is applied to avoid workpiece shaping errors resulting from GWAS edge wear. When openings of a minor length are considered, the role of the working

time of the GWAS zones that do not contact the workpiece surface could be significant. This issue, schematically represented in Fig. 1, affects the traverse and the reciprocating grinding. In the plunge grinding process with or without oscillations, the material removal rate is not dependent on the grinding wheel path in the axial direction, but rather in the radial direction (v_{fr}); therefore, introduction of the corrective index for such kinematic variations is not necessary.

For traverse grinding (Fig. 1a), the formula describing the material removal rate should include the time during which the grinding wheel, with a given axial table feed speed v_{fa}, has to move along the workpiece with a grinding wheel height $c_s = T$, after which the contact between the GWAS and the workpiece ends. The movement length l_t of the grinding wheel in such a process is calculated as follows:

$$l_t = b_w + c_s = b_w + T, \text{mm}; \tag{13}$$

where:

b_w workpiece width;
c_s grinding wheel coasting, mm.

Therefore, the traverse grinding material removal rate should be determined using the corrective index k_t, detailed below:

$$k_t = \frac{b_w}{(b_w + c_s)} = \frac{b_w}{(b_w + T)}, -. \tag{14}$$

In reciprocating grinding (Fig. 1b), the total passage l_r of the grinding wheel along the ground surface should include double the value of the assumed coasting c_s, since the coasting occurs on both sides of the ground opening:

$$l_r = b_w - T + 2c_s, \text{mm}. \tag{15}$$

Another factor that causes discrepancies in the values of momentary and actual material removal rates in the reciprocating grinding process is the number of passes i_p in the axial direction occurring between subsequent additions of the radial table feed value f_r. This is observed when the total working engagement $a_{e\ tot}$ is divided into numerous working passes, during which the speed v_{fa} and the values of elementary engagements a_e are directed radially f_r in a discontinuous manner. Below is a formula determining the corrective coefficient k_r for the reciprocating grinding process, taking into consideration the grinding wheel coasting c_s and the number of passes i_p:

$$k_r = \frac{1}{i_p} \cdot \frac{b_w}{(b_w - T + 2c_s)}, -. \tag{16}$$

Table 2 shows kinematic diagrams of the internal cylindrical grinding processes, the formulae presented in relevant scientific literature defining the material removal rate Q_w (4, 6) the formulae containing the corrective indexes k_t (14) and k_r (16), and the relationships defining the material removal rate $Q_{w\ cor}$ (17–19).

The dependences defining the corrected material removal rate $Q_{w\ cor}$ were the basis of further analyses to determine the index describing the GWAS active grains load.

3 Number of the kinetic cutting edges N_{kin}

The dependences (17–19) described above determine the corrected material removal rate during a given grinding operation. The durability period of the grinding wheel is highly dependent on the working conditions of the abrasive grains. To calculate the load per single active grain (taking part in the machining), the number of active (kinematic) cutting vertexes N_{kin} per 1 mm^2 of the GWAS had to be assessed using the following formula [7]:

$$N_{\text{kin}} = A \cdot C_{st1}^{\beta} \left(\frac{v_w}{v_s}\right)^{\alpha} \cdot \left(\frac{a_e}{d_{\text{eq}}}\right)^{\frac{\alpha}{2}}, \text{mm}^{-2}; \tag{20}$$

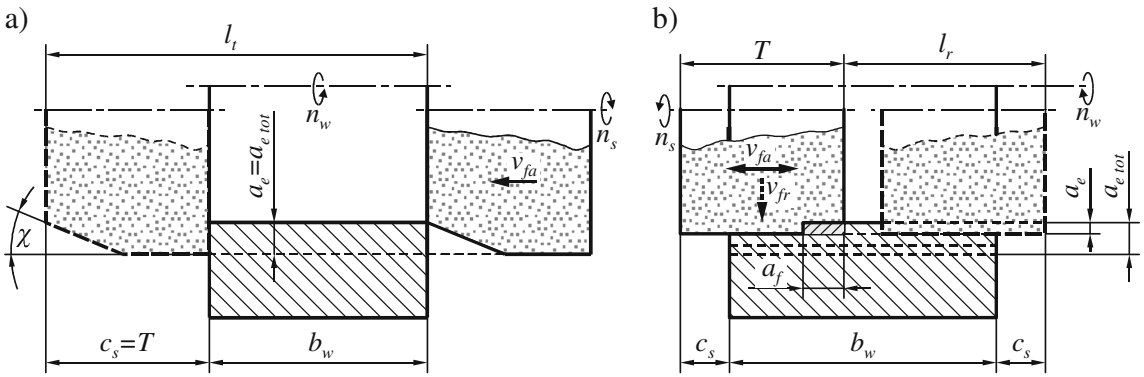

Fig. 1 Effect of the grinding wheel coasting c_s on the length of grinding wheel displacement in the axial direction. **a** traverse grinding l_t. **b** Reciprocating grinding l_r

Table 2 Calculation formulae for the material removal rate Q_w

	Traverse grinding	Reciprocating grinding	Plunge grinding	Plunge grinding with osccillations
Grinding process kinematic scheme	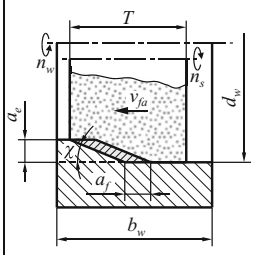	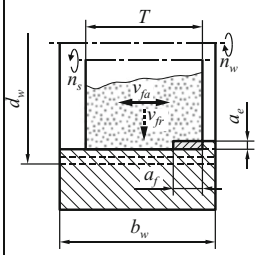	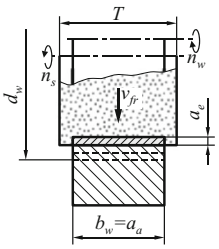	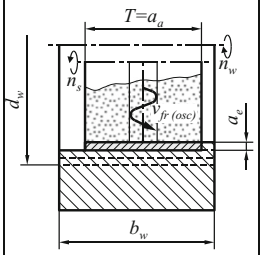
Material removal rate Q_w, mm³/s	$Q_w = \pi \cdot d_w \cdot a_e \cdot a_f \cdot n_w$		$Q_w = \pi \cdot d_w \cdot a_a \cdot a_e \cdot n_w$	
Correction coefficient	$k_t = \frac{b_w}{(b_w + c_s)}$ where: $c_s = T$	$k_r = \frac{1}{i_p} \cdot \frac{b_w}{(b_w - T + 2c_s)}$ where: $c_s = \frac{T}{3}$	–	
Corrected material removal rate ($Q_{w\,cor} = Q_w \cdot k$) $Q_{w\,cor}$, mm³/s	$Q_{w\,cor} = \pi \cdot d_w \cdot n_w \cdot \cdot a_f \cdot a_e \cdot \frac{b_w}{(b_w+T)}$ (17)	$Q_{w\,cor} = \pi \cdot d_w \cdot n_w \cdot \cdot a_f \cdot a_e \cdot \frac{1}{i_p} \cdot \frac{b_w}{\left(b_w - \frac{T}{3}\right)}$ (18)	$Q_{w\,cor} = Q_w$ (19)	

where:

A proportionality constant, −;
C_{st1} static cutting edge density on depth z (z—working zone depth), mm^{-3};
α, β exponential coefficients based on cutting edge distribution on the GWAS (α, $\beta > 0$), −.

The equivalent grinding wheel diameter d_{eq}, present in formula (20), is described as having a dependence (12). The proportionality constant A was calculated on the basis of the following formula (21):

$$A = \frac{1}{1+\alpha} \cdot 1,6^{3\alpha}, -. \tag{21}$$

Static cutting edges density C_{st1} was determined in accordance with the following formula (22):

$$C_{st1} = \frac{N_{st}}{z^q}, \text{mm}^{-3}; \tag{22}$$

where:

N_{st} the number of static edges, −;
z working zone depth, mm.

The exponential coefficient α occurring in the formula used to calculate the proportionality constant A (21) was determined on the basis of formula (23) and the assumption that the exponential coefficient values are $p \approx 2$ and $q \approx 1$, as described in the relevant literature:

$$\alpha = \frac{q}{p+1}, -. \tag{23}$$

To define the kinetic values of the cutting edges N_{kin}, the number of static edges N_{st} in formula (22) must also be determined. In the analysis described here, the N_{st} value was calculated from the GWAS microtopography measurement. It was assumed that the number of static cutting edges was equivalent to the *Sds* parameter value, which describes the surface vertexes density. This assumption was confirmed by the peak count histogram of the GWAS (Fig. 2b). Figure 2a shows example values of the grinding wheel active surface geometric structure parameters (*Sa*, *St* and *Sds*) after filtering the tool's cylindrical shape and levelling the microtopography. Figure 2c presents the SEM image of the active surface of the grinding wheel, which was made of microcrystalline sintered corundum grains and glass-crystalline ceramic bond (1–35 × 20 × 10-SG/F46K7VDG).

The N_{kin} value determined as described above was multiplied by the grinding wheel active surface area A_{GWAS} to obtain the number of cutting vertexes on the GWAS, marked as $N_{kin\,GWAS}$, in accordance with formula (24):

$$N_{kin\,GWAS} = N_{kin} \cdot A_{GWAS}, -; \tag{24}$$

where:

$$A_{GWAS} = \pi \cdot d_s \cdot T, \text{mm}^2. \tag{25}$$

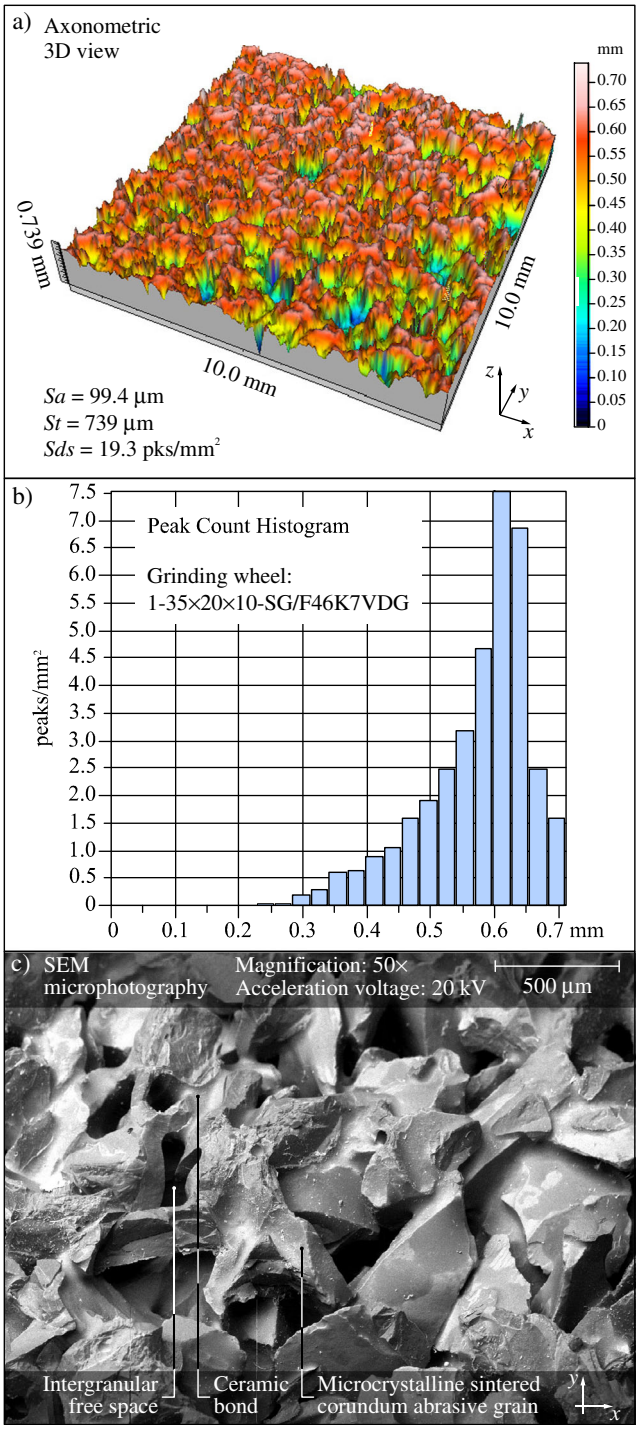

Fig. 2 Example of a grinding wheel active surface. **a** GSS parameters and axonometric 3D view of levelled microtopography. **b** Peak count histogram of the GWAS. **c** SEM microphotography

4 The synthetic index of single abrasive grain material removal rate SI_Q

The synthetic index of single abrasive grain material removal rate SI_Q was defined as a corrected material removal rate $Q_{w\ cor}$ divided by the number of active cutting edges on the GWAS $N_{\text{kin GWAS}}$ and by the ratio of speed q, in accordance with the following formula:

$$SI_Q = \frac{Q_{w\ cor}}{N_{\text{kin GWAS}} \cdot q}, \mu\text{m}^3/\text{s}. \tag{26}$$

Next, a formula describing the material removal rate per single active cutting edge, expressed in mm^3/s, was obtained. Relating this value to the ratio of speed q, defined as:

$$q = \frac{v_s}{v_w}, -, \tag{27}$$

allowed the inclusion of changes in the chips' cross-section resulting from alterations in the grinding wheel and workpiece speed.

Taking into account dependences (24), (25) and (27), the final formula for calculating the SI_Q coefficient assumes the following form:

$$SI_Q = \frac{Q_{w\ cor} \cdot v_w}{N_{\text{kin}} \cdot \pi \cdot d_s \cdot T \cdot v_s}, \mu\text{m}^3/\text{s}. \tag{28}$$

In the case of traverse and reciprocating grinding, the SI_Q coefficient described as above is sensitive to changes in the following grinding parameters: a_e, v_s, v_w, v_{fa}, N_{kin}, d_s, d_w, and T. In the kinematics of plunge grinding and plunge grinding with oscillations, the SI_Q coefficient values depend on: a_e, v_s, v_w, v_{fr}, N_{kin}, d_s, d_w, and T. This feature makes the SI_Q coefficient highly useful in selecting machining parameters in situations that require the active grains load to remain constant, particularly when changing the internal cylindrical grinding process kinematics. It also demonstrates how the load of the active cutting edges changes during the functioning of the above-mentioned machining parameters and allows their optimal selection.

5 An example of the SI_Q index results

Examplative results of calculations of the SI_Q synthetic coefficient values for the discussed kinematic variations of internal cylindrical grinding are presented in Table 3. The table includes intermediate size values necessary for determining the value of SI_Q, as well as the values of the assumed grinding parameters and the exponential coefficients.

Figure 3 presents charts describing the variability of SI_Q values calculated for traverse (Fig. 3a, b), reciprocating (Fig. 3c, d) and plunge (Fig. 3e) grinding processes, in accordance with formula (28) for the machining parameters variability range exemplified (a_e, v_{fa}, v_{fr}, v_s i v_w). The remaining

Table 3 Example calculation results of the SI_Q index, with all input data for considered kinematic variants of the internal cylindrical grinding process

Parameter	Example results			
	Traverse grinding	Reciprocating grinding	Plunge grinding	Plunge grinding with osccillations
Material removal rate Q_w, mm^3/s (4), (6)	50.27	9.42	7.54	7.54
Corrected material removal rate $Q_{w\,cor}$, mm^3/s (17–19)	23.81	7.48	7.54	7.54
Proportionality constant A, − (21)	1.20	1.20	1.20	1.20
Static cutting edges N_{st}, mm^{-2} (from the GWAS microtopography)	19.3	19.3	19.3	19.3
Static cutting edge density on depth z = 1 mm C_{st1}, mm^{-3} (22)	26.12	26.12	26.12	26.12
Kinetic cutting edges N_{kin}, mm^{-2} (20)	2.17	1.22	0.82	0.82
Kinetic cutting edges on the GWAS $N_{kin\ GWAS}$, − (24)	4782.16	2683.90	1794.56	1794.56
Synthetic index of single abrasive grain material removal rate SI_Q, μm^3/s (28)	62,236.44	34,857.83	52,518.73	52,518.73
Grinding parameters and exponential coefficients	v_s = 60 m/s d_s = 35.0 mm T = 20.0 mm v_w = 0.75 m/s n_w = 5.97 s^{-1} d_w = 40.0 mm b_w = 18.0 mm A_{GWAS} = 2199.11 mm^2 a_a = − $a_f = v_{fa}/n_w$ = 0.34 mm $a_e = a_{e\,tot}$ = 0.20 mm $a_{e\,tot}$ = 0.20 mm v_{fa} = 2.0 mm/s v_{fr} = − i_p = − α = 1/3 β = 1 $p \approx 2$ $q \approx 1$ z = 0.739 mm	v_s = 60 m/s d_s = 35.0 mm T = 20.0 mm v_w = 0.75 m/s n_w = 5.97 s^{-1} d_w = 40.0 mm b_w = 18.0 mm A_{GWAS} = 2199.11 mm^2 a_a = − $a_f = v_{fa}/n_w$ = 2.01 mm $a_e = 0.0125/i_p$, mm $a_{e\,tot}$ = 0.20 mm v_{fa} = 12 mm/s v_{fr} = − i_p = 2 α = 1/3 β = 1 $p \approx 2$ $q \approx 1$ z = 0.739 mm	v_s = 60 m/s d_s = 35.0 mm T = 20.0 mm v_w = 0.75 m/s n_w = 5.97 s^{-1} d_w = 40.0 mm b_w = 18.0 mm A_{GWAS} = 2199.11 mm^2 $a_a = b_w$ = 18.0 mm a_f = − $a_e = v_{fr}/n_w$ = 0.00056 mm $a_{e\,tot}$ = 0.20 mm v_{fa} = − v_{fr} = 0.0033 mm/s i_p = − α = 1/3 β = 1 $p \approx 2$ $q \approx 1$ z = 0.739 mm	v_s = 60 m/s d_s = 35.0 mm T = 20.0 mm v_w = 0.75 m/s n_w = 5.97 s^{-1} d_w = 40.0 mm b_w = 18.0 mm A_{GWAS} = 2199.11 mm^2 $a_a = b_w$ = 18.0 mm $a_f = v_{fa}/n_w$ = 2.01 mm $a_e = v_{fr}/n_w$ = 0.00056 mm $a_{e\,tot}$ = 0.20 mm v_{fa} = 12 mm/s v_{fr} = 0.0033 mm/s i_p = − α = 1/3 β = 1 $p \approx 2$ $q \approx 1$ z = 0.739 mm

grinding parameters and values of the power coefficients were assumed to be in concord with the data presented in Table 3.

As the charts in Fig. 3 show, for constants N_{kin}, d_s, d_w, b_w and T, values of the synthetic coefficient of As the charts in Fig. 3 show values of the synthetic coefficient of material removal rate per single cutting edge SI_Q for the constants N_{kin}, d_s, d_w, b_w and T are directly proportional to a_e, v_{fa}, v_{fr} and v_w, and inversely proportional to v_s, which results from the construction of formula (28).

The SI_Q coefficient can determines the active grains load in the grinding process by taking into consideration the eight grinding parameters enumerated in Section 4. Figure 4 shows an exemplary application of coefficient SI_Q in calculating the grinding parameters within which the grain load reaches a different level in different kinematic variants. Values corresponding to the exemplary coefficient value $SI_Q \approx 62{,}000$ μm^3/s are marked in the charts by yellow dots.

The example illustrated in Fig. 4 shows that it is possible to select the grinding parameters using the SI_Q coefficient for various process kinematics, so as to maintain a comparable abrasive grain load on the grinding wheel active surface. The charts' shape is the basis for modifying the appropriate machining parameters taking into consideration the active grains load too. Application of the SI_Q coefficient can also predict the working conditions of grinding wheels with different numbers of active grains on their GWAS, as determined by the method presented in Section 3.

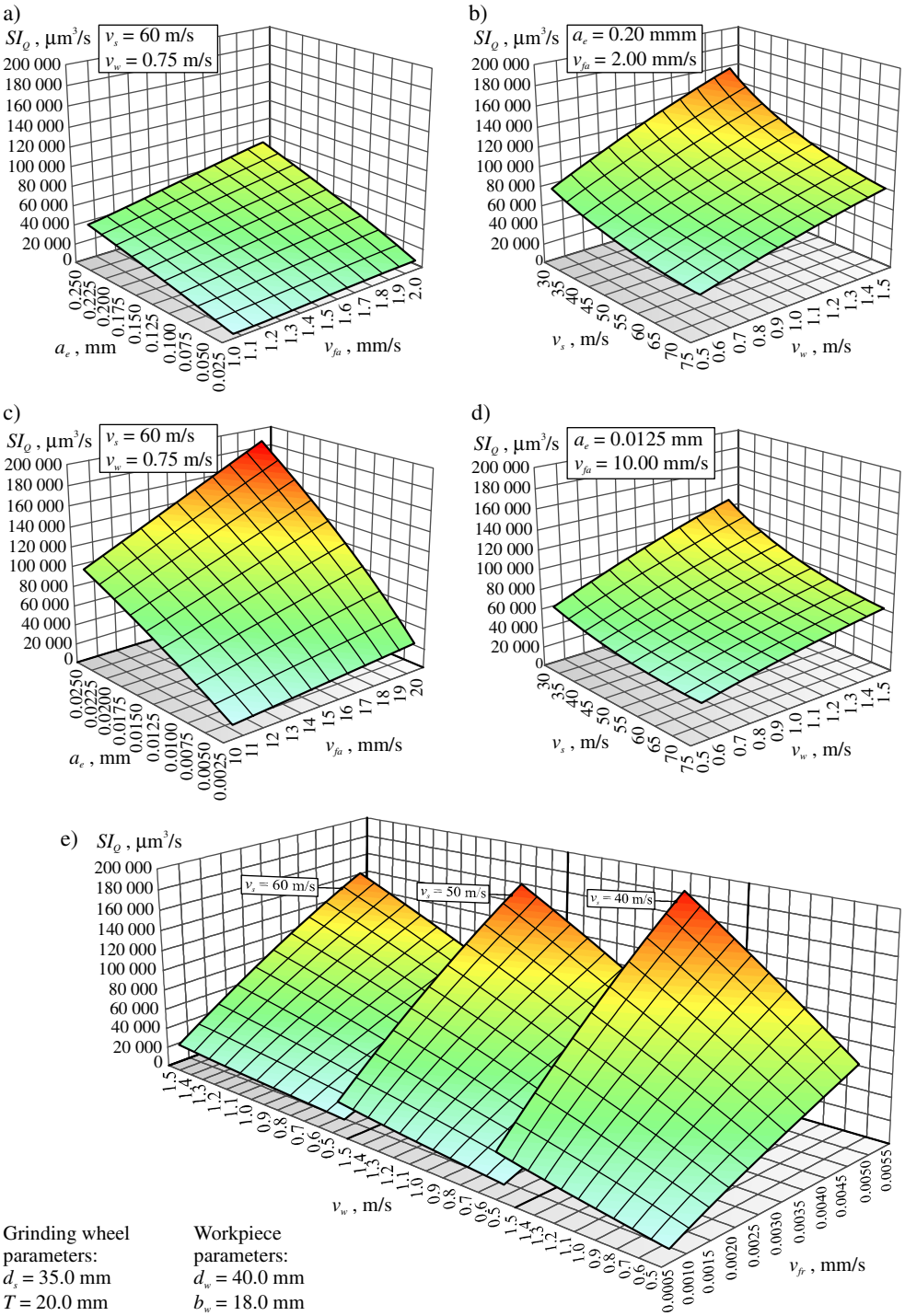

Fig. 3 Diagrams of the SI_Q index example values for **a**, **b** traverse grinding; **c**, **d** reciprocating grinding; **e** plunge grinding

Grinding wheel parameters:
d_s = 35.0 mm
T = 20.0 mm

Workpiece parameters:
d_w = 40.0 mm
b_w = 18.0 mm

6 Experimental verification of the SI_Q index applicability

Because of the difficulty in determining the actual number of contacts occurring in the grinding zone, experimental verification of the acquired values of the SI_Q is very difficult. The grinding wheel has an undefined geometry of cutting edges that results from the random geometry of the abrasive grains and their random distribution in the volume of the tool. Therefore, even on the same grinding wheel, the different active surface portions show a significant scattering of the statistical parameters describing the state of GWAS (such as the number vertex per mm^2 *Sds*, the total height of the surface *St*, or distribution of vertexes–abrasive grains), which largely depend on the dressing parameters and

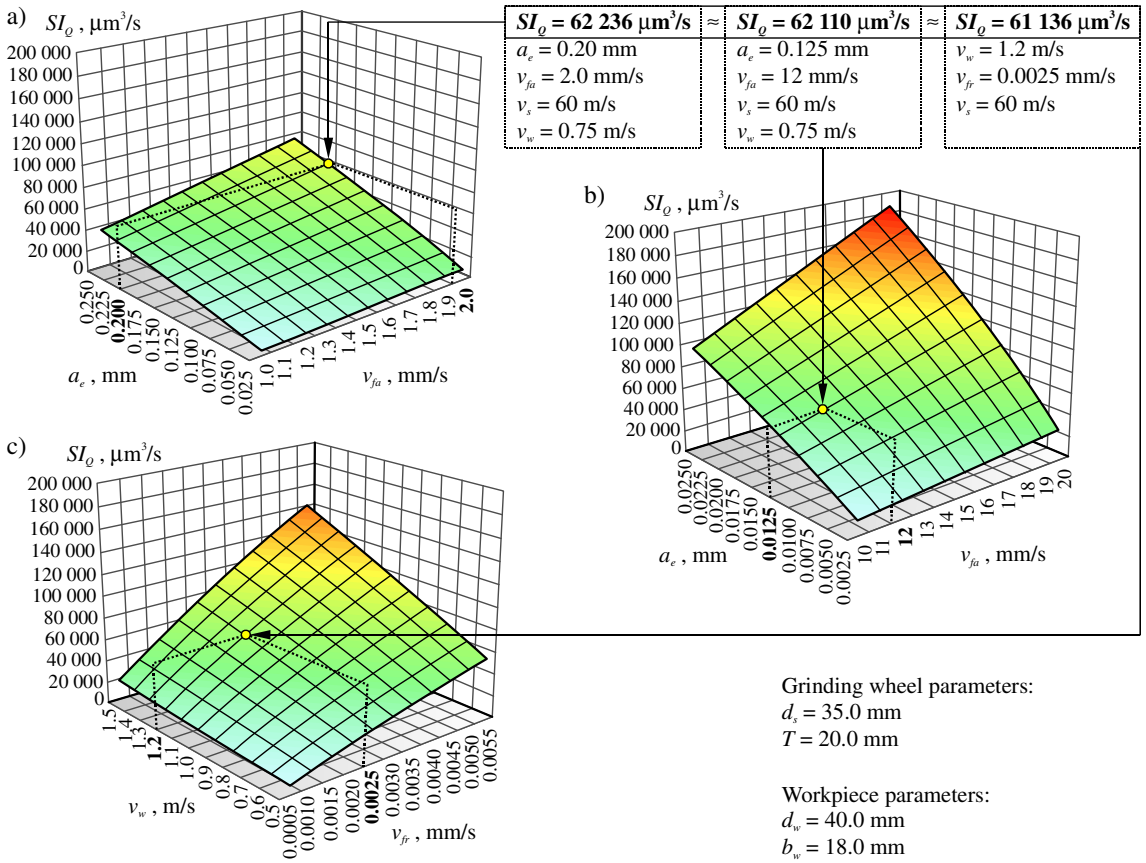

Fig. 4 The determination of grinding parameters for which abrasive grain loads are at a comparable level, using the SI_Q index. **a** Traverse grinding. **b** Reciprocating grinding. **c** Plunge grinding

Table 4 Grinding conditions

Machine	Universal grinding machine RUP 28P by Mechanical Works Tarnow SA, Poland, equipped with spindle type EV-70/70-2WB produced by Fisher, Switzerland (max. Rpm 60,000 min^{-1}, power of machine cutting 5.2 kW)					
Dressing conditions	Single diamond dresser; dresser weight Q_d = 1.25 kt n_{sd} = 12,000 min^{-1}, v_{fd} = 10 m/s, a_d = 0.0125 mm					
Process	Traverse internal cylindrical grinding			Plunge internal cylindrical grinding		
Grinding wheel	1–35 × 20 × 10-SG/F46K7VDG with conic chamfer (χ = 0.72°; b = 16 mm)			1–35 × 20 × 10-SG/F46K7VDG		
Constant parameters of grinding	$a_e = a_{e\ tot}$ = 0.20 mm v_{fa} = 20 mm/s v_s = 60 m/s Q_C = 5.0 L/min			$a_{e\ tot}$ = 0.20 mm v_{fa} = 20 mm/s v_{fr} = 0.0025 mm/s v_s = 60 m/s Q_C = 5.0 L/min		
Variable parameters of grinding	v_w = 0.6 m/s	v_w = 0.75 m/s	v_w = 1.0 m/s	v_w = 1.0 m/s	v_w = 1.2 m/s	v_w = 1.5 m/s
***SI*$_Q$**	**53,634 µm³/s**	**62,236 µm³/s**	**75,394 µm³/s**	**52,519 µm³/s**	**61,136 µm³/s**	**73,630 µm³/s**
Coolant	5 % water solution of Castrol Syntilo RHS oil given by flood method					
Workpiece	Internal cylindrical surface of bearing rings, made of 100Cr6 steel (63 ± 2 HRC), internal diameter: d_w = 40 mm, width: b_w = 18 mm					

a_d dressing allowance, mm; b grinding wheel conic chamfer width, mm; n_{sd} grinding wheel rotational speed while dressing, min^{-1}; v_{fd} axial table feed speed while dressing, mm/s; Q_d diamond dresser mass, kt; Q_C grinding fluid flow rate, L/min; χ angle of the grinding wheel conic chamfer, °

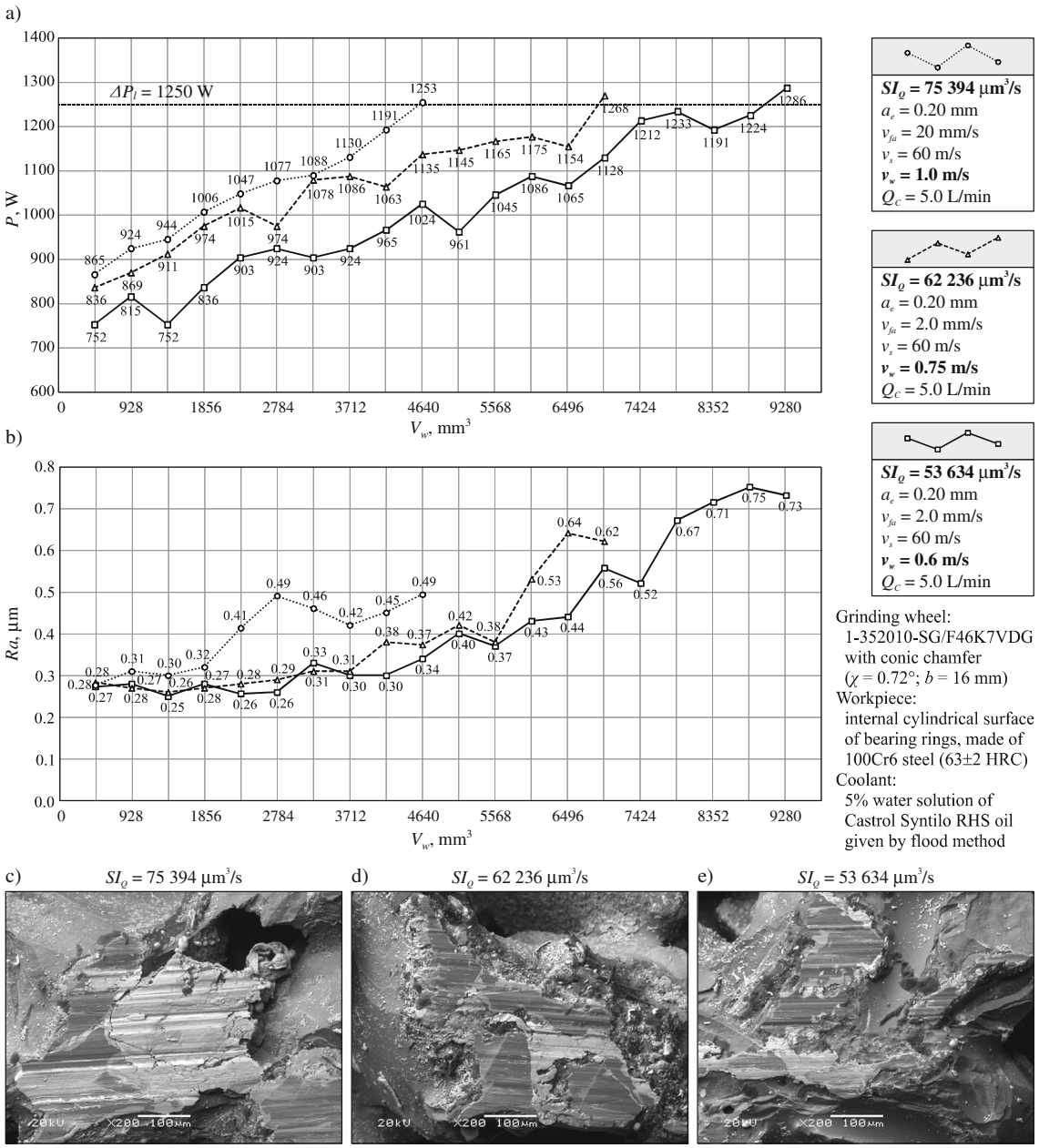

Fig. 5 Changes of values of the selected process parameters over material removal V_w during traverse internal cylindrical grinding as well as SEM microscopic images of the wheels after machining. **a** grinding power gain ΔP. **b** Arithmetic mean deviation of the workpiece profile *R*a **c** GWAS after grinding with SI_Q = 75,394 μm³/s. **d** GWAS after grinding with SI_Q = 62,236 μm³/s. **e** GWAS after grinding with SI_Q = 53,634 μm³/s

phenomena associated with the wear of abrasive grains and vitrified bond bridges. These considerations were taken into account, including the geometric parameters describing the state of the active surface of the measured grinding wheel–covered by the analysis in Section 3. The actual number of active vertexes were dynamically changed during the process, due to wear of abrasive grains and crumbling of bond bridges. Also, for small-sized grinding wheels (e.g. d_s = 35 mm) the number of contacts is very high (for v_s = 60 m/s it is approximately 550 per second, and the duration of a single contact with the machined surface is approximately 10^{-5} s). All these aspects make an experiment aimed the capturing of one microchip originating from a single contact of the cutting tip of a single abrasive grain extremely difficult, especially in the internal cylindrical grinding process, which is characterized by a long contact zone between the grinding wheel and machined

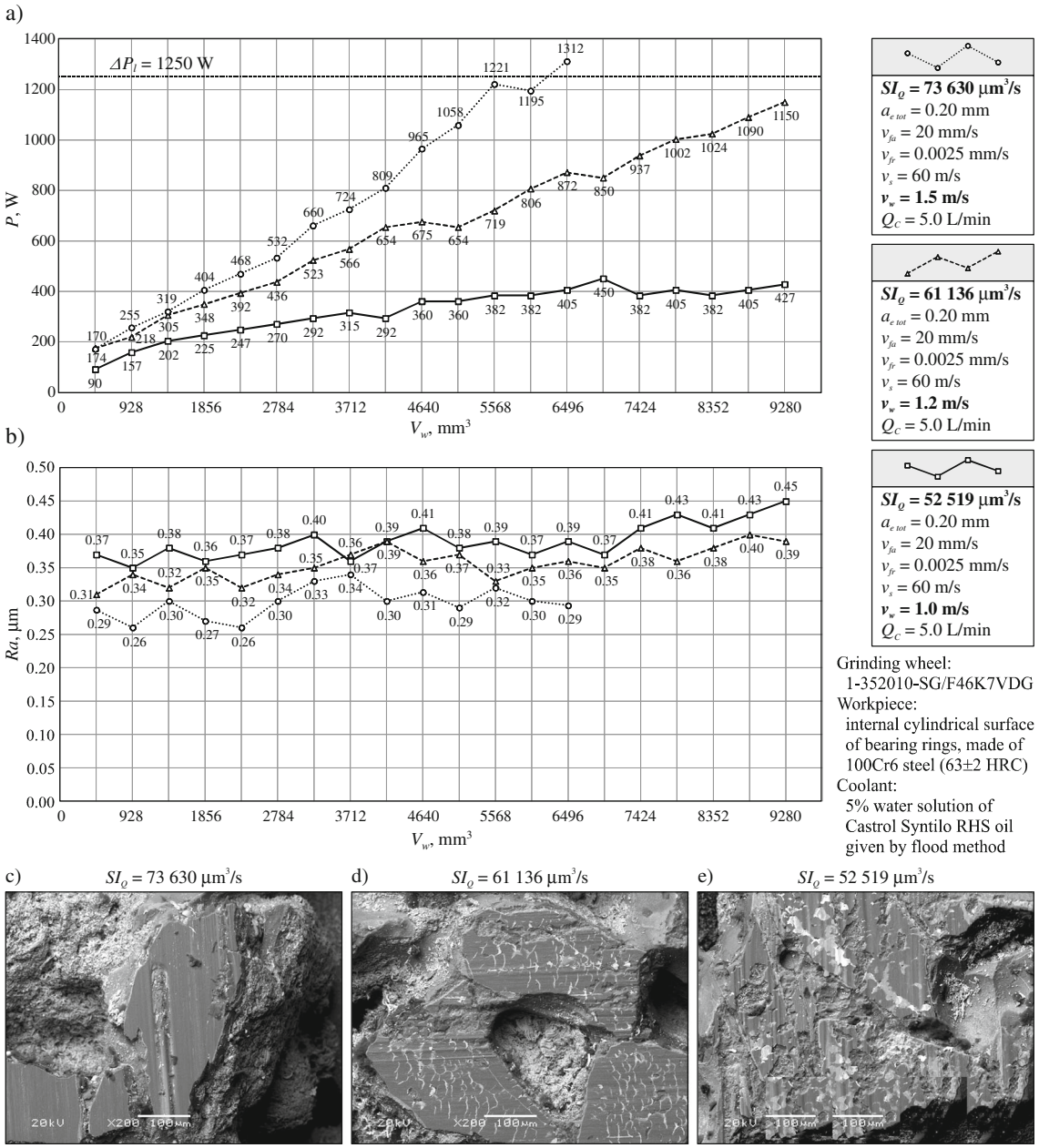

Fig. 6 Changes of values of the selected process parameters over material removal V_w during plunge internal cylindrical grinding as well as SEM microscopic images of the wheels after machining. **a** grinding power gain ΔP. **b** arithmetic mean deviation of the workpiece profile *R*a. **c** GWAS after grinding with SI_Q = 73,630 µm³/s. **d** GWAS after grinding with SI_Q = 61,136 µm³/s. **e** GWAS after grinding with SI_Q = 52,519 µm³/s

surface and by difficult access to the grinding zone. Many studies are concerned with microcutting with a single abrasive grain, but in them, the allowance is usually much larger than in the actual grinding process using a grinding wheel. Hence, the emphasis is placed on the use of analytical and simulation methods for the analysis of elementary phenomena in grinding.

For the reasons presented above, rather than a direct experimental investigation of the ground material's volume determined by a single cutting tip, an attempt to indirectly verify the applicability of the proposed index SI_Q was made.

6.1 Methodology of experimental tests

Changes in grinding power *P* and machined surface roughness *R*a (arithmetic mean deviation of the workpiece roughness profile in µm) were recorded during the removal of 9280 mm³ of the workpiece. This corresponded to the grinding of 20 subsequent rings with the parameters shown in Table 4. The grinding wheel was dressed prior to machining the first opening. Based on exploratory research, the end-life of the examined grinding wheels was set at the limit value of grinding power gain ΔP_l = 1250 W.

The recorded variations in the parameters resulted from the progressive wear of the GWAS. Tempo, scale and dominant phenomenon of the GWAS wear largely depend on the load of cutting vertex, which describes the SI_Q index. Therefore, it was assumed that changes in the parameters describing the course and results of grinding (P and Ra) and the state of the GWAS after testing (analysis of SEM images of the GWAS) were sufficient to verify the applicability of the SI_Q index.

As a variable parameter of grinding adopted the workpiece peripheral speed v_w. Specific v_w values were chosen to obtain SI_Q values ~10,000 μm^3/s larger or smaller than the ones given in the example in Fig. 4 (≈62,000 μm^3/s). The study was conducted in two kinematic varieties of internal cylindrical grinding: traverse and plunge grinding. The same grinding wheels were used in all tests (characterized previously in Fig. 2), except in the traverse grinding, where a conic chamfer was shaped on the GWAS (with an angle χ = 0.72° and width b = 16 mm) [12]. Modifying the geometry of the wheel caused a slight increase in the grinding wheel active surface area A_{GWAS}, which was included in the calculation.

The surface roughness parameters of the grinded rings were determined on the basis of the profiles registered using the stylus profilometer Hommel-Tester T8000 by Hommelwerke GmbH (Germany). The GWAS microscopic images were taken with the scanning electron microscope JSM-5500LV by JEOL Ltd. (Japan).

6.2 Experiments results and discussion

Figure 5 shows the variations in the grinding power gain ΔP (Fig. 5a) and the arithmetic mean deviation of the workpiece profile Ra (Fig. 5b) over the material removal V_w during traverse internal cylindrical grinding. The diagrams demonstrate that a decrease in SI_Q values (resulting from changes in the value of v_w) results in a longer grinding wheel life. There is a clear correlation between the values of grinding power gain ΔP and the SI_Q index (Fig. 5a).

Similar results were observed in the plunge grinding process (Fig. 6a). In both kinematic varieties of grinding, the surface roughness remained at the same level with no clear effect caused by the different machining conditions (Fig. 5b and Fig. 6b).

SEM microscopic images of the wheels after machining using different conditions (Fig. 5c–e and Fig. 6c–e) reveal clear differences in the abrasive grains active vertexes. Grinding with the highest value of the SI_Q index (SI_Q = 75,394 μm^3/s for traverse grinding and SI_Q = 73,630 μm^3/s for plunge grinding) was characterized by no self-sharpening and renewal of the cutting abilities of the grinding wheels made of microcrystalline sintered corundum. The wear was most probably caused by the friction between the workpiece and abrasive grain and by the abrasive grains' plastic flow at high temperature and pressure. This possibility is sustained by the presence of large smooth surfaces in contact areas and by the loads of intergranular free spaces visible in the SEM images (Fig. 5c and 6c). Such wear phenomena caused a short grinding wheel life and an off-limit value of the grinding power ΔP_l (Fig. 5a and 6a). Increasing of the grain load (SI_Q = 62,236 μm^3/s for traverse grinding and SI_Q = 61,136 μm^3/s for plunge grinding) partially exposed new cutting micro-vertexes on the dulled surface of abrasive grains, as can be seen in Fig. 5d and 6d. The most favourable grinding condition was obtained at the smallest load of abrasive grains: SI_Q = 53,634 μm^3/s for traverse grinding and SI_Q = 52,519 μm^3/s for plunge grinding. SEM microscopic images in Fig. 5e and 6e show clear signs of micro-fracture of dulled grain fragments and progressive self-sharpening of the GWAS. In these conditions, the longest life and lowest grinding power increase was recorded for the grinding wheels used in the experiments (Fig. 5a and 6a). Therefore, it can be concluded that in this case, there was a larger share of the abrasive grains' fracture wear caused by mechanical and thermal shock loads as well as fatigue and thermal-fatigue wear induced by the recurrent mechanical shock load. These conditions stimulated the exposure of new, sharp cutting micro-vertexes on the GWAS.

Analysis of the experimental results indicate that despite the use of different kinematics of grinding processes and machining parameters induce similar changes in measured values. Variability in the values corresponded to changes in the SI_Q index. This suggests that the working conditions of a grinding wheel and grinding results obtained in one kinematic variation can be recreated in a different internal cylindrical grinding process when the SI_Q index is used. Therefore, the index can be applied as a general criterion for the selection of grinding parameters.

7 Conclusions

The most important conclusions resulting from the analyses of the kinematic parameters of the internal cylindrical grinding process are as follows:

- Study of the available literature concerning the kinematic parameters of the grinding process revealed the need to define a new index which would synthetically refer to all the key grinding parameters, and the geometric structure of the grinding wheel active surface
- In definition (28) of the new coefficient, named SI_Q (synthetic index of single abrasive grain material removal rate), the material removal rate Q_w is related to the number of active grains on the GWAS and the reverse q speed ratio.

- the SI_Q coefficient allows comparison between different kinematic variants of the internal cylindrical grinding process.
- The dependence defining SI_Q takes into account changes in the following grinding parameters: a_e, v_s, v_w, v_{fa}, N_{kin}, d_s, d_w, and T (in traverse and reciprocating grinding) and a_e, v_s, v_w, v_{fr}, N_{kin}, d_s, d_w, and T (in the kinematics of plunge grinding with and without oscillations).
- The SI_Q coefficient offers the possibility of selecting the machining parameters when the internal cylindrical grinding process kinematics have changed and the active grains load must remain at the same level (as shown in Section 6).
- Because SI_Q values can be used to determine changes in the load of active cutting edges in relation to other parameters, the index can be used to optimize the selection of various machining parameters.
- The SI_Q coefficient can be used when knowledge of the influence of the machining parameters on the abrasive grains working conditions, and the resulting grinding wheel wear intensity, is necessary.
- By using the SI_Q coefficient, it is now possible to compare grinding wheels with a different GWAS geometric structure. This facilitates the recreation of specific operating conditions (including wear and self-sharpening of the grinding wheel active surface, obtained from a previous grinding wheel with different GSS) through proper selection of the most important machining parameters.
- The SI_Q coefficient allows for prediction of the working conditions of grinding wheels with different number of active grains on the GWAS.
- Introduction of the corrective indexes k_t (14) and k_r (16) into the formulae describing the material removal rate Q_w makes the SI_Q coefficient easy to apply in laboratory tests and also in industrial practice.

References

1. Marinescu ID, Rowe WB, Dimitrov B, Inasaki I (2004) Tribology of abrasive machining processes. William Andrew, Norwich
2. Marinescu ID, Hitchiner M, Uhlmann E, Rowe WB, Inasaki I (2007) Handbook of machining with grinding wheels. CRC Press, Boca Raton
3. Rowe WB (2009) Principles of modern grinding technology. William Andrew, Burlington
4. Klocke F (2009) Manufacturing processes 2: grinding, honing, lapping. Springer-Verlag, Berlin
5. Yamada K, Ueda T, Hosokawa A (2011) A study on aspects of attrition wear of cutting grains in grinding process. Int J Precis Eng Manuf 12(6):965–973
6. ISO 3002–5: (1989) Basic quantities in cutting and grinding. Part 5: basic terminology for grinding processes using grinding wheels
7. Klocke F, Hegener G (1999) Schnell, gut und flexibel: Hochleistungs-Aussenrund-Formschleifen. IDR 33(2):153–160
8. Weinert K, Finke M, Kötter D (2003) Wirtschaftliche Alternative zum Hartdrehen. Innenrund-Schälschleifen steigert Flexibilität beim Schleifen von Futterteilen. Maschinenmarkt 109(48):44–47
9. Tönshoff HK, Karpuschewski B, Mandrysch T, Inasaki I (1998) Grinding process achievements and consequences on machine tools challenges and opportunities. CIRP Ann 47(2):651–668
10. Webster J, Tricard M (2004) Innovations in abrasive products for precision grinding. CIRP Ann 53(2):597–617
11. Slowinski B, Nadolny K (2007) Effective manufacturing method for automated inside diameter grinding. J Adv Mech Des Syst 1(4): 472–480
12. Nadolny K (2013) A review on single-pass grinding processes. J Cent South Univ T 20:1502–1509
13. Nadolny K (2013) Microdiscontinuities of the grinding wheel and their effects on its durability during internal cylindrical grinding. Mach Sci Technol 17:74–92